# 1

# Electrochemical Pore Array Fabrication on n-Type Silicon Electrodes

V. Lehmann
*Infineon Technologies AG, Dept. CPS EB BS, Otto-Hahn-Ring 6, D-81730 München, Germany*
*volker.lehmann@infineon.com*

## 1.1. WHY THE FIRST ARTIFICIAL PORE ARRAYS WERE REALIZED IN N-TYPE SILICON ELECTRODES

The surface morphology of a solid-state electrode after an electrochemical dissolution process depends sensitively on the parameters of anodization. The one extreme case is an anodization condition under which even a rough electrode surface becomes homogeneously smooth, this process has been termed electropolishing. If in contrast the surface becomes rougher, we deal with corrosion or pore formation. In the prior case, commonly the crevice geometry is random and no narrow size regime is observed. This is different in the latter case. Electrochemically formed porous materials usually show a narrow pore size distribution and a certain pore density, which allows us to determine the ratio of pore volume to the total volume, the porosity. In most cases, the pore distribution at the electrode surface is random; however, in certain cases, like for example, for porous alumina, a short-range order may be observed. Pore arrays with a long-range order of the pore positions, which are desirable for a multitude of applications, can only be produced artificially.

The fact that n-type silicon was the first electrode material on which pore arrays of such a long-range order have been realized is not purely accidental. For artificial patterning, the electrochemical pore initiation process must be understood and a structuring technique must be available. In many electrode–electrolyte systems, the pore initiation mechanism is complex and still under debate, as for example, for pore formation in aluminium [1]. In other systems, like alumina, the pore size is small and just becomes

assessable for today's most advanced structuring technologies [2]. In contrast, in low-doped n-type silicon electrodes, to a large extent, the pore initiation is simply controlled by the interface topography and the pore size is well measured in the micrometre regime. This enabled us about a decade ago to use the standard silicon process technology available at that time, such as thin film deposition, photolithography, and wet etching, to generate a pore initiation pattern. Upon anodization in hydrofluoric acid (HF) this arbitrary pattern developed into an array of straight pores [3]. The resulting pore morphology can be inspected by cleaving the silicon electrode and subsequent optical microscopy (OM) or scanning electron microscopy (SEM).

Over the years, the electrochemical etching process has been optimized and today the pore array may cover a whole silicon wafer and penetrate its full thickness. Furthermore, pore arrays have been realized by the anodization of a multitude of other materials as discussed in subsequent chapters.

## 1.2. THE PHYSICS OF PORE INITIATION ON SILICON ELECTRODES IN HF

In order to predetermine the position of an electrochemically formed pore a detailed understanding of the pore initiation process is required. The pore initiation may, for example, be dominated by the impurity or defect distribution, by the state of electrode passivation, or by the topography of the electrode surface. As a consequence, structuring techniques for electrochemical pore array fabrication could be based on local impurity implantation, depassivation, or etching of depressions to generate pore initiation sites.

For the case of n-type silicon an anodic oxide has been discussed as a potential candidate for passive film formation. An indispensable constituent of all electrolytes for pore formation in silicon electrodes, however, is hydrofluoric acid, which readily dissolves $SiO_2$. Pore initiation by defects is unlikely as well, because today's silicon crystals are manufactured free of defects and with atomic impurity levels down to $10^{12}$ $cm^{-3}$. The third of the above options, the topography of the electrode surface, has been found to be the relevant factor for the pore initiation process.

All pore formation on silicon electrodes is observed in an anodic regime where the dissolution reaction is limited by charge supply from the electrode. This regime is characterized by an anodic current density below a critical value $J_{PS}$. $J_{PS}$ depends on electrolyte concentration, temperature and crystal orientation of the electrode [4]. The dissolution reaction is initiated by a hole (defect electron), reaching the silicon–electrolyte interface. Since charge supply is the limiting factor dissolution occurs preferentially at sites which attract holes. If no such sites are present, like for example, for an atomically flat electrode the dissolution starts homogeneously. However, any inhomogeneity of dissolution will be amplified and within seconds etch pits are formed, which act as initiation sites for pore growth. This random pore initiation process at polished electrode surfaces is shown in Figure 1.1. Note that in the first 30 seconds of anodization a very high density of nanometre-sized etch pits are generated. In the next 30 seconds, a few of these pits increase their size by a factor of 5 or more consuming neighbouring pits. This process continues until the number of surviving pores becomes constant. This is the case, after about 240 seconds, for an n-type doping concentration of $10^{16}$ $cm^{-3}$.

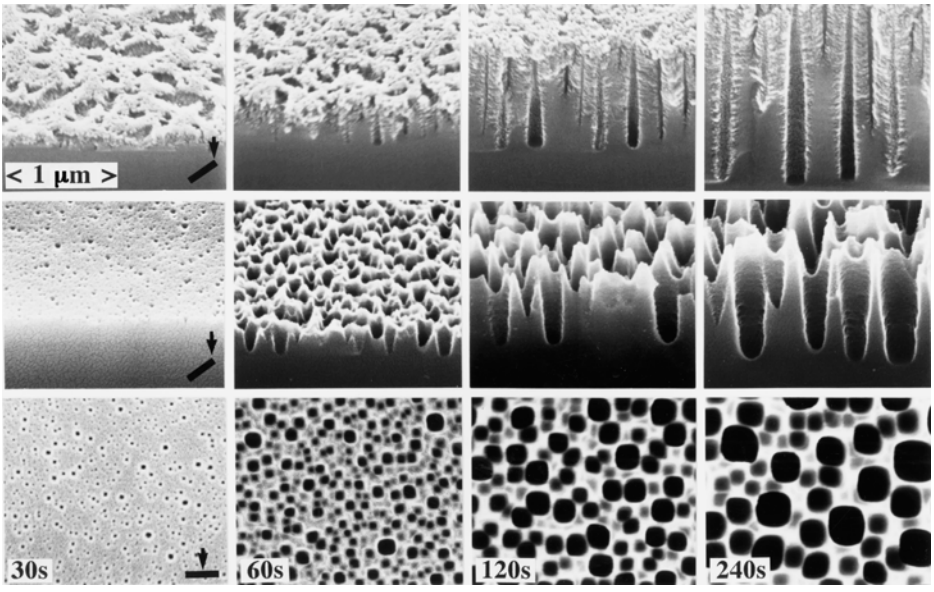


FIGURE 1.1. SEM micrographs of spontaneous pore initiation on polished surfaces of n-type Si electrodes anodized for the indicated times under white light illumination of the front side (14 V, 2.5% HF, 10 mA/cm$^{-2}$, n-type Si $10^{16}$ cm$^{-3}$ (100)). Microporous silicon covering the macropores, as shown on the top row (cross-sectional view), has been removed by alkaline etching for better visibility at centre (cross-sectional view) and the bottom row (surface view). From Ref. [1].

If depressions are already present in the electrode prior to anodization, it is easily understood that they become initiation sites for the pore formation. A pattern of artificial initiation sites works only as desired, if its pitch is close to the pore spacing that develops spontaneously on the silicon electrode upon anodization. The average distance of random pores is usually in the same order of magnitude as the pore diameter. The observed diameters of pores formed in silicon electrodes cover four orders of magnitude and is classified in three size regimes. A porous film is designated microporous if the pore diameter is below 2 nm. In this size regime, pore formation is dominated by quantum size effects. While the pore size becomes mesoporous (2 nm $<$ pore diameter $<$ 50 nm) or macroporous (pore diameter $>$ 50 nm) if the formation process is dominated by the electric field in the space–charge region (SCR). In the electric field dominated case, the morphology of the porous structure depends sensitively on the way the charge carriers pass through the SCR. An overview of the different size regimes and the proposed pore formation mechanism is displayed in Figure 1.2. The fact that the pore initiation site can be predetermined by a depression in the electrode surface has first been shown for macropores in low-doped n-type electrodes for which the pore formation is dominated by minority carrier collection. Later on, however, it has been shown that for the other three field-dominated pore formation effects, as displayed in Figure 1.2, a depression is as well sufficient as initiation site [5]. Figures 1.3b–d show arrays of macropores on p-type silicon, the pores initiate preferentially at the pyramidal depression in the pre-structured electrode surface. Figure 1.3e shows a minute mesopore formed by tunnelling of charge

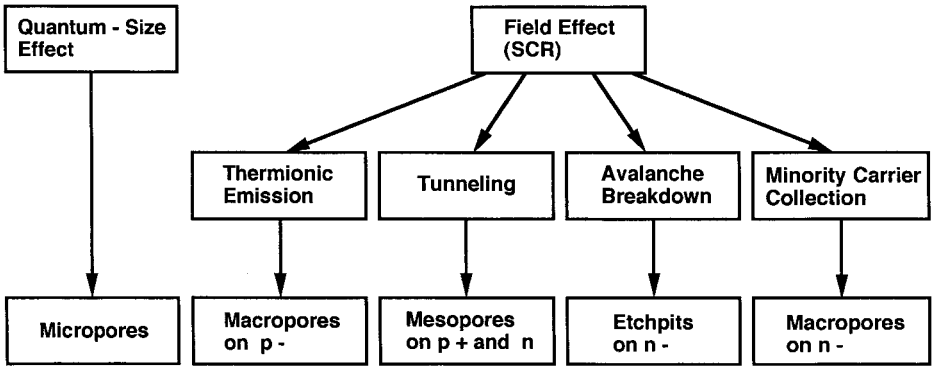


FIGURE 1.2. Effects proposed to be responsible for pore wall passivation (top row). Effects which can lead to passivation breakdown at the pore tip (middle row) and the resulting kind of porous silicon structure together with substrate doping type (bottom row). From Ref. [5].

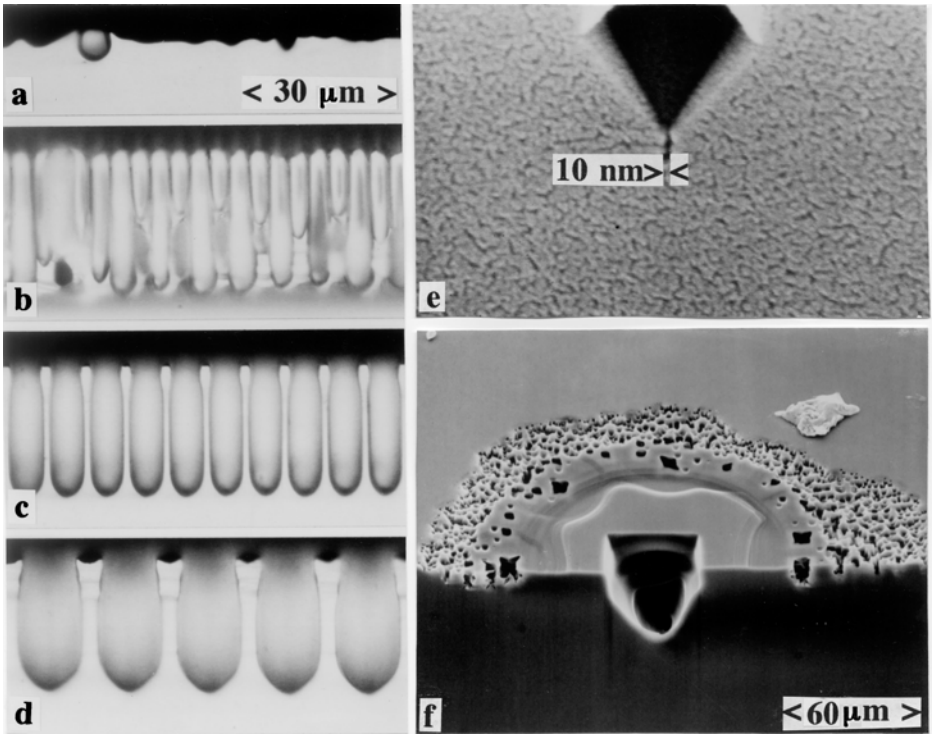


FIGURE 1.3. Electrochemical pore formation in silicon electrodes of different kinds and density of doping initiated by an artificial depression. (a–d) Pore initiation on a polished (a) and on patterned (b–d) p-type silicon electrodes (2 mA/cm$^2$, 3% HF, 240 minutes, p-type Si $3 \times 10^{14}$ cm$^{-3}$) (OM after [6]). (e) Mesopore formation at the tip of a pyramidal etch pit (10 V, 6% HF, 5 seconds, n-type Si $10^{15}$ cm$^{-3}$) (SEM after [4]). (f) A large circular etch pit structure formed by avalanche breakdown (50 V, 6% HF, 100 seconds, n-type Si $10^{15}$ cm$^{-3}$). Note that the structure is centred around the pyramidal initiation etch pit (SEM from Ref. [5]).

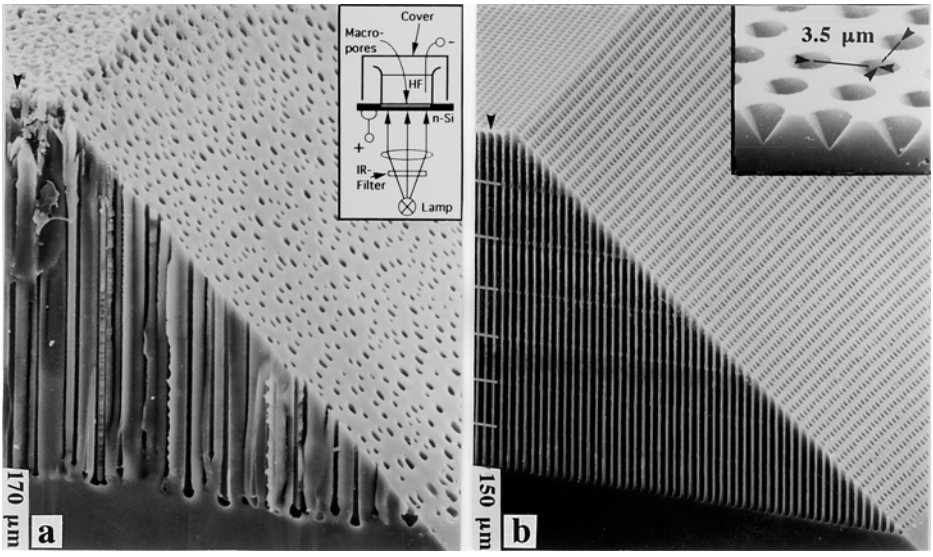


FIGURE 1.4. SEM micrographs of surface, cross section and a 45° level of anodized n-type silicon samples ($10^{15}$ cm$^{-3}$). Sample (a) shows randomly distributed pores due to anodization of a polished electrode, while sample (b) shows a square array of pores generated by anodization of a patterned surface. The pore initiation pattern, as shown in the inset, has been produced by photolithography and alkaline etching. From Ref. [4].

carriers located at the tip of a depression. Figure 1.3f shows that a large cavity formed by avalanche breakdown is also centred at the tip of an artificial depression. It can be speculated that even the initiation of micropores is sensitive to the electrode topology. In order to test this hypothesis, however, the required resolution of the initiation pattern has to be in the order of 1 nm and is therefore beyond today's photolithographic structuring techniques.

The density of random pores in n-type silicon electrodes decreases with decreasing substrate-doping density. For an n-type doping concentration of $10^{15}$ cm$^{-3}$, as shown in Figure 1.4a, the pore initiation process takes longer and the final pore density is lower, as for example shown for an n-type doping concentration of $10^{16}$ cm$^{-3}$ in Figure 1.1. This dependence of pore density on the doping level of the bulk silicon reflects the influence of the SCR width on the formation process of initiation sites. A depression produces a deformation of the SCR and the electric field becomes maximum where the radius of curvature of the depression has its minimum. For the case of highly doped silicon the electric field easily reaches its breakdown value even for moderate applied bias if the tip radius is reduced to a few tens of nanometres. As a consequence, the tunnelling of charge carriers is confined to the tip of the depression. In low-doped silicon, where the field strength is usually below the breakdown value, the transfer of charge carriers is still influenced by the topography and shows a maximum at the tip of the depression. Even if the field of the SCR is neglected and pure hole diffusion is considered, a depression is still a favourable location for charge transfer. In the case of low-doped n-type silicon electrodes the electric field as well as the diffusion have to be considered for pore initiation and pore growth [5,6].

In conclusion, a flat silicon electrode anodized in HF below the critical current density is unstable. Such a system shows a tendency to enhance inhomogeneities of the surface topography. An artificial pore initiation pattern realized by depression in the electrodes surface exploits this instability to form pore arrays. An example of such a pore array is shown in Figure 1.4b. The array of etch pits used for initiation is shown in the inset of this figure.

## 1.3. THE PHOTOLITHOGRAPHIC PRE-STRUCTURING PROCESS AND THE ANODIZATION SET-UP

A depression, sufficient for pore initiation in an n-type electrode, can be realized in many ways. Most compatible with today's semiconductor manufacturing techniques is photolithographic structuring. The basic process sequence is sketched in Figure 1.5. A thermal oxide is formed on a polished, (100)-oriented, n-type silicon wafer with a highly doped n-type backside layer. A photoresist is then deposited on the front side and illuminated using a mask with the desired pore pattern. Subsequently windows in the oxide film are opened, using a plasma etch process, for example. A wet alkaline etching

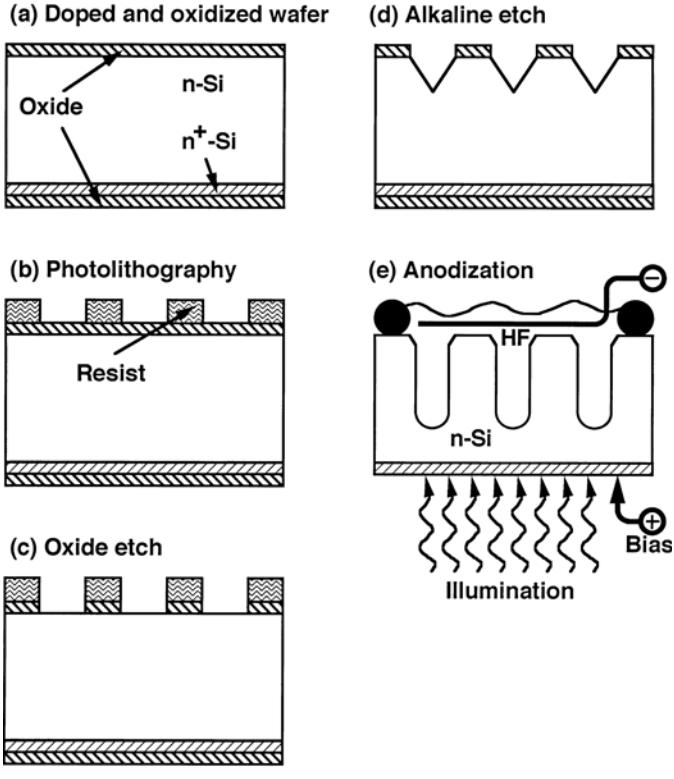


FIGURE 1.5. Schematic view of the fabrication process of pore arrays in n-type silicon electrodes.

process then generates sharp-tipped etch pits that show the geometry of an inverted pyramid, as shown in the inset of Figure 1.4b. These etch pits act as initiation sites for the electrochemical etching process, because their collection efficiency for holes (defect electrons), generated by illumination of the electrode backside, is much better than the one for the flat substrate.

The pore initiation process is sensitive to the geometry of the depression. For a depression with a large radius of curvature at the bottom, for example, the starting position of the pore is badly defined. As a consequence, a certain mispositioning of the pores in an array can be expected. An inverted pyramid with a flat bottom, for example, can be realized by a reduction of alkaline etching time. For such a geometry, the formation of four pores located at the four corners of the inverted pyramid bottom has been observed.

The electrolyte used for macropore array formation in n-type Si electrodes is composed of aqueous HF. The pore growth rate depends sensitively on HF concentration (commonly 1–10%) and is in the order of 1 μm/min. Hydrogen is a by-product of the electrochemical dissolution process. In order to reduce the sticking probability of hydrogen bubbles to the electrode surface, addition of a detergent and strong electrolyte agitation are recommended. PVC or PP is recommended as materials for the cell body. Standard O rings (nitrile polymer) are found to be stable in the HF electrolyte. A platinum electrode is commonly used as cathode. A reference electrode is not required because the pore formation process on n-type silicon is not very sensitive to bias. The highly doped backside electrode is connected to the positive side of the power supply, collecting the photo-generated electrons.

The light source used for illumination of the n-type electrode should emit at wavelengths below 900 nm, because longer wavelengths penetrate deep into the bulk and might generate charge carriers in the pore walls. Such light sources can be realized by LEDs or by a filament lamp with an optical short-pass filter.

## 1.4. LIMITING FACTORS AND DESIGN RULES FOR MACROPORE ARRAYS ON N-TYPE SILICON ELECTRODES

Not all desirable macropore array geometries can be realized by the electrochemical etching process. This section gives the upper and lower limits for pore dimensions and a few design rules [7].

The realization of a desired pore pattern requires a certain doping density of the n-type Si electrode. A good rule of thumb for the selection of an appropriate substrate is to multiply the desired pore density given (in $\mu m^2$) by $10^{16}$ and take this number as doping density (in $cm^{-3}$). This dependency is shown in Figure 1.6. A square pattern of 10 μm pitch, for example, produces a pore density of 0.01 pores/$\mu m^2$ which can be best etched using a substrate of an n-type doping density of $10^{14}$ $cm^{-3}$. A maladjustment of pore pattern and substrate doping density will lead to branching of pores, as shown in Figure 1.7a or dying of pores, as shown in Figure 1.7c.

The number of possible arrangements of the pore pattern is only limited by the requirement that under homogeneous backside illumination the porosity has to be constant on a length scale above about three times the pitch. This means it is possible to etch a

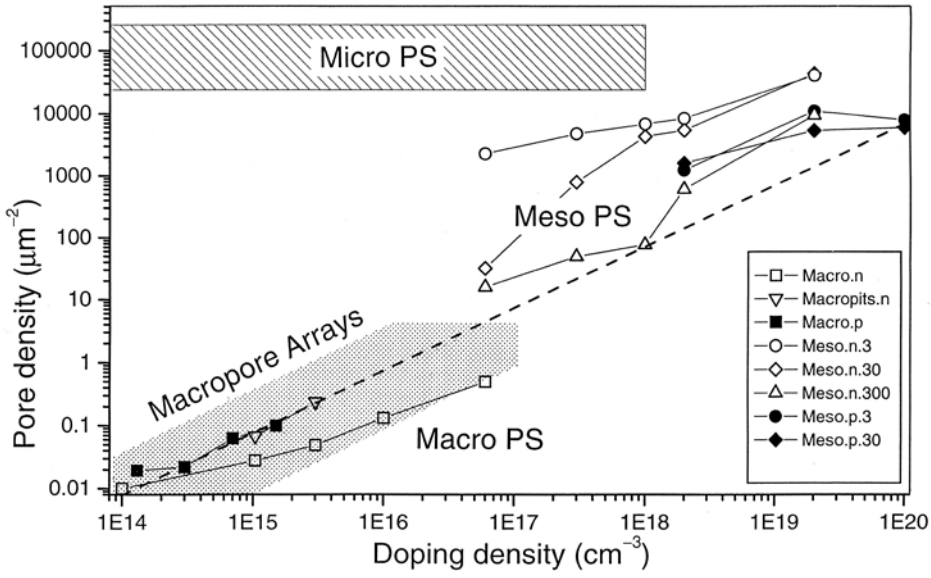


FIGURE 1.6. Pore density versus silicon electrode doping density for porous silicon layers of different size regimes. The dashed line shows the pore density of a triangular pore pattern with a pore pitch equal to two times the SCR width for 3 V applied bias. Note that only macropores on n-type substrates may show a pore spacing significantly exceeding this limit. The regime of stable macropore array formation on n-type Si is indicated by a dot pattern. Type of doping and the formation of current density (in mA/cm$^2$) are indicated in the legend. From Ref. [5].

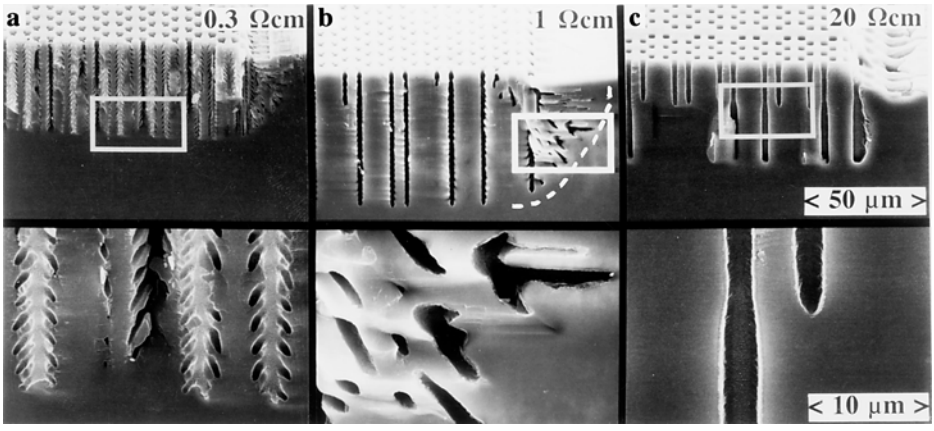


FIGURE 1.7. SEM micrographs of macropore array morphology for the same initiation pattern applied to differently doped n-type electrodes (2.5% HF, 5 mA/cm$^2$, 2 V). (a) For the highly doped electrode the pitch of the pattern is too coarse, which leads to branching. (c) For the low-doped substrate the pattern is too fine which results in dying of pores. (b) Doping density and pitch are well adjusted in this case and branching is only observed at the border to an unpatterned area (underetching indicated by white dashed line). From Ref. [7].

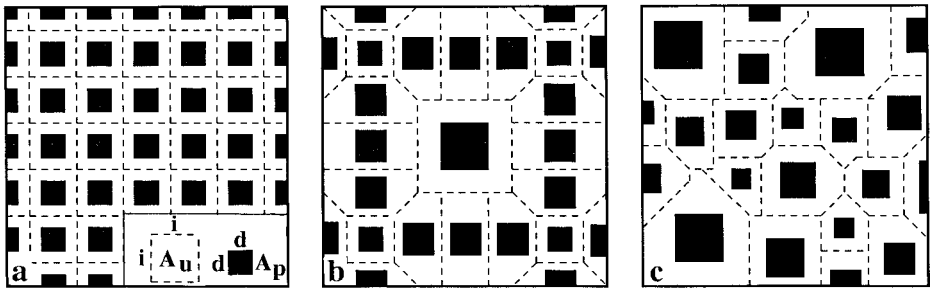


FIGURE 1.8. Sketches showing cross sections of macropore arrays orthogonal to the growth direction (a) for a square, (b) for an ordered and (c) for a random pattern. The pores (black squares) collect holes from the area indicated by the dashed lines. The porosity (the ratio of the black area to the total area) is 0.25 for all patterns.

pattern with a missing pore, a missing row of pores or even two missing rows. Patterns as shown in Figure 1.8b can also be etched. A single pore, however, cannot be etched. It is also possible to enlarge or shrink the pitch of a pattern across the sample surface by a maximum factor of about 3. But a pattern with an abrupt border to an unpatterned area will lead to severe underetching according to Figure 1.7b and random pore formation in the unpatterned area.

A local variation of porosity can be produced by an inhomogeneous illumination intensity. However, any image projected on the backside of the wafer generates a smoothed-out current density distribution on the front side, due to random diffusion of the charge carriers in the bulk. This problem can be reduced if thin wafers or illumination of the front side is used. However, sharp lateral changes of porosity cannot be realized.

Arrays with pore diameters $d$ as small as about 0.3 μm have been realized [7]. The lower limit for the pore diameter of an ordered array is established by breakdown, which leads to light-independent pore growth and spiking. There seems to be no upper limit for the pore diameter, because the formation of 100 μm wide pores has been shown to be feasible [8]. Array porosities may range from 0.01 to close to 1. The porosity, which is controlled by the etching current, determines the ratio between the pore diameter and the pitch of the pore pattern. This means for a square pattern, any pore diameter between one-tenth of the pitch and nearly the pitch can be realized.

The pore diameter can be varied over the length of the pore by a factor up to about 3 for all pores simultaneously by adjusting the current density, as visualized by Figure 1.9. This means the porosity normal to the surface can be varied. The taper of such pore geometries is limited by dying of pores to values below about 30° for a pore diameter decreasing in growth direction, while values in the order of 45° have been realized for an increase of pore diameter in growth direction [9]. Note that narrow bottlenecks will significantly reduce the diffusion in the pore and the formation of deep modulated pores becomes more difficult than the formation of straight pores. Bottlenecks at the pore entrance may result from the transition of the pyramidal etch pit into a pore tip. They can be avoided by an increase of the current density during the first minutes of pore array fabrication.

The pore cross section under stable array formation conditions is usually a rounded square, as shown in Figure 1.10b. Subsequent to electrochemical pore formation, the cross section can be made round by oxidation steps or can be made square by chemical

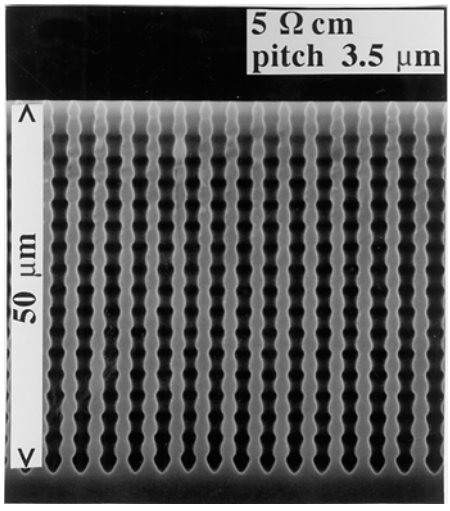


FIGURE 1.9. A sine wave modulation of the etching current versus etching time produces an array of macropores with corresponding modulation of a diameter. From Ref. [7].

etching at RT in aqueous HF or weak alkaline solutions such as diluted KOH or $NH_4OH$. The formation of side pores by branching or spiking, as shown in Figure 1.7a, can be suppressed by an increase of current density or a decrease of doping density, bias or HF concentration. The dying of pores, as shown in Figure 1.7c, is suppressed by an increase of current density, doping density or bias.

The pore length $l$ can be as large as the wafer thickness (up to 1 mm). However, the growth of deep pores requires low electrolyte concentrations, low temperatures and etching times in the order of a day or more, because the etch rate in deep pores is limited by HF diffusion to values in the order of 0.5 μm/min and below. Shorter pores ($l < 0.1$ mm) can be etched much faster (5 μm/min). Under stable etching conditions all pores have the same length. Pore arrays with through-pores can be realized by an increase of the etching current density into the electropolishing regime, which separates a free-standing porous plate from the substrate. Macropores penetrating the whole wafer thickness can be etched as well, however, pore formation becomes unstable in the vicinity of the backside. The formation of dead-end pores and subsequent oxidation and alkaline etchback has found to be technologically favourable.

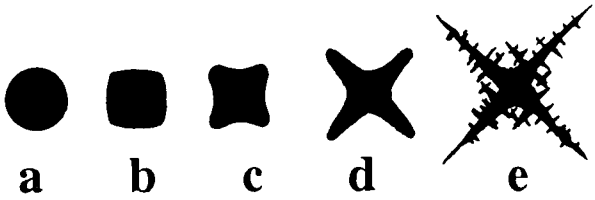


FIGURE 1.10. By an increase of bias or doping density the round (a) or slightly faceted (b) cross section of macropores becomes star shaped by branching (c and d) or spiking (e) along the ⟨100⟩ directions orthogonal to the growth direction.

Another effect which limits the obtainable pore length is characterized by a sudden drop of the growth rate at the pore tip to negligible values and an increase of pore diameter close to the tip. This degradation of pore growth establishes an upper limit for the pore length for a given set of anodization parameters. The fact that pore degradation is delayed for a reduced formation current, which produces conical pores is an indication for a diffusion related phenomenon. The observed dependence of degradation on the concentration of the dissolution product $H_2SiF_6$ in the electrolyte points to a poisoning of the dissolution reaction. The maximum obtainable pore depth decreases rapidly with increasing HF concentration. This effect has been ascribed to the rate of $H_2SiF_6$ production being proportional to $J_{PS}$ which again depends exponentially on HF concentration, while the diffusion of $H_2SiF_6$ is expected to show little dependence on HF concentration [7].

The pore growth direction is along the $\langle 100 \rangle$ direction and toward the source of holes. For the growth of perfect macropores perpendicular to the electrode surface (100)-oriented Si substrates are required. Tilted pore arrays can be etched on substrates with a certain misorientation to the (100) plane. Misorientation, however, enhances the tendency of branching and angles of about $20^\circ$ seem to be an upper limit for unbranched pores.

In conclusion, it can be said that the limits of macropore array formation are in some way complementary to the limitations of plasma etching. The latter technique gives a higher degree of freedom in lateral design, while the freedom in vertical design and the feasible pore aspect ratios is limited.

Today's applications of macropore arrays range from electronic applications such as capacitors to optical filters and biochips.

## REFERENCES

[1] T. Martin and K.R. Hebert, Atomic force microscopy study of anodic etching of aluminum, J. Electrochem. Soc. **148**, B101–B109 (2001).
[2] H. Masuda and K. Fukuda, Science **268**, 1466 (1995).
[3] V. Lehmann and H. Föll, Formation mechanism and properties of electrochemically etched trenches in n-type silicon, J. Electrochem. Soc. **137**, 653–659 (1990).
[4] V. Lehmann, R. Stengl and A. Luigart, On the morphology and the electrochemical formation mechanism of mesoporous silicon, Mater. Sci. Eng. B **69–70**, 11–22 (2000).
[5] V. Lehmann, The physics of macropore formation in low doped n-type silicon, J. Electrochem. Soc. **140**, 2836–2843 (1993).
[6] V. Lehmann and S. Rönnebeck, The physics of macropore formation in low doped p-type silicon, J. Electrochem. Soc. **146**, 2968–2975 (1999).
[7] V. Lehmann and U. Grüning, The limits of macropore array fabrication, Thin Sol. Films **297**, 13–17 (1997).
[8] P. Kleinmann, J. Linnros and S. Peterson, Formation of wide and deep pores in silicon by electrochemical etching, Mater. Sci. Eng. B **69–70**, 29–33 (2000).
[9] F. Müller, A. Birner, J. Schilling, U. Gösele, C. Kettner and P. Hänggi, Membranes for micropumps from macroporous silicon, Phys. Status Solidi a **182**, 585 (2000).